Cell. Mol. Biol. (ISSN: 1165-158X)

Journal Homepage: www.cellmolbiol.org

Cellular and Molecular Biology

Original Article

TMAO converts cytochrome c into a pro-apoptotic peroxidase by destabilizing the heme-Met80 ligation

Kuldeep Singh[1], Anju Kumari[1], Seemasundari Yumlembam[2], Nelson Mutum[1], Radhika Bakhshi[3,4], Prachi Rani[1], Kajal Mavi[1], Akshita Gupta[1*], Laishram Rajendrakumar Singh[1*]

[1] Dr. B. R. Ambedkar Center for Biomedical Research, University of Delhi, Delhi-110007, India
[2] Manipur University, Department of Botany, 795004, Imphal, India
[3] Institute of Home Economics, University of Delhi, Delhi, India
[4] Shaheed Rajguru College of Applied Sciences for Women, University of Delhi, Delhi, India

Article Info

Article history:

Received: October 02, 2025
Accepted: December 05, 2025
Published: December 31, 2025

Use your device to scan and read the article online

Abstract

Trimethylamine N-oxide (TMAO), a gut microbiota–derived metabolite, has been linked to cardiovascular, renal, and hepatic disorders, but its direct impact on mitochondrial apoptotic machinery remains unclear. Here, we show that TMAO binds cytochrome c (Cyt c), disrupting its structural integrity and converting it into an apoptotically competent species. Spectroscopic analyses revealed that TMAO destabilizes the heme–Met80 axial ligation, shifting Cyt c from its native hexacoordinate to a pentacoordinate state. This conformational change enhances peroxidase activity, exposes hydrophobic clusters, and perturbs the Trp microenvironment, marking Cyt c's transition from electron carrier to pro-apoptotic catalyst. Absorption spectra further showed splitting of the native 530 nm band into peaks at 520 and 550 nm, consistent with heme reduction. These alterations facilitate Cyt c release from the mitochondrial membrane and engagement in intrinsic apoptosis. Given that TMAO accumulates at higher concentrations in tissues enriched with oxygen transporters, such as kidney and liver, our findings provide mechanistic insight into its role in organ-specific toxicity, including chronic kidney disease (CKD) and non-alcoholic fatty liver disease (NAFLD). This study establishes a direct molecular link between TMAO and mitochondrial apoptosis via Cyt c destabilization, suggesting that stabilizing Cyt c could represent a therapeutic strategy against TMAO-associated pathologies.

Keywords: TMAO, Apoptosis, Cytochrome C, Heme, Peroxidase

1. Introduction

The interplay between diet, the gut microbiome, and host metabolism has emerged as a critical determinant of health and disease. Within this meta-organismal axis, Trimethylamine N-oxide (TMAO) has been consistently identified as a key metabolite associated with adverse cardiometabolic outcomes. Nutritional precursors such as choline, phosphatidylcholine (lecithin), L-carnitine, and betaine are metabolized by gut microbial enzymes, including choline TMA-lyase (cutC) and carnitine oxidoreductase (cntAB), to generate trimethylamine (TMA). This intermediate is subsequently oxidized by hepatic flavin-containing monooxygenase 3 (FMO3) to form TMAO [1-3]. Elevated systemic TMAO levels are strongly correlated with cardiovascular diseases, atherosclerosis, and heart failure, suggesting its role as an active mediator rather than a passive biomarker of disease progression [4-6]. The underlying mechanisms of these pathologies involve enhanced oxidative stress, chronic inflammation, and activation of apoptotic pathways[7]. TMAO is believed to contribute to these processes through direct interactions with proteins and receptors central to cellular homeostasis. For example, TMAO activates protein kinase R-like endoplasmic reticulum kinase (PERK), initiating an unfolded protein response cascade characterized by eIF2α phosphorylation, ATF4 induction, and CHOP upregulation, ultimately leading to apoptosis[8,9]. In addition, TMAO has been shown to interact with carbonic anhydrases, thereby perturbing CO_2 hydration and acid–base homeostasis, which exacerbates vascular oxidative stress [10]. TMAO also influences endothelial nitric oxide synthase (eNOS) activity, impairing nitric oxide production and promoting vascular dysfunction through increased oxidative burden[11]. Further interactions with proteins such as lipases and bovine serum albumin (BSA) indicate that the pathological impact of TMAO is multifaceted and extends across several molecular pathways[12].

A critical downstream target of TMAO-mediated cellular stress is Cyt c, a small heme protein that resides in the mitochondrial intermembrane space. Under normal conditions, Cyt c functions as an electron carrier between complexes III and IV of the respiratory chain and is stabilized

* Corresponding author.
E-mail address: lairksingh@gmail.com (L. R. Singh); akshi.398@gmail.com (A. Gupta).
Doi: http://dx.doi.org/10.14715/cmb/2025.71.12.13

in a hexacoordinate heme configuration, where the heme iron is ligated by His18 and Met80. During oxidative or apoptotic stress, weakening of the Met80–heme bond drives Cyt c toward a pentacoordinate state, activating its peroxidase function and facilitating its release from the inner mitochondrial membrane to the cytosol, where it triggers caspase activation and intrinsic apoptosis [13–17].

Given the established link between TMAO and apoptosis, we hypothesized that TMAO may directly interact with Cyt c and alter its structure and redox state. Therefore, this study combines spectroscopic, biochemical, and computational approaches to examine whether TMAO binding drives Cyt c toward an apoptotically competent conformation.

2. Materials and methods

2.1. Materials

Trimethylamine N-oxide (TMAO), potassium chloride (KCl), potassium dihydrogen phosphate (KH_2PO_4), and dipotassium hydrogen phosphate (K_2HPO_4) were procured from Merck. Cytochrome c (bovine heart) and all other chemicals, unless otherwise specified, were obtained from Sigma-Aldrich. Thioflavin T (ThT) and 8-anilinonaphthalene-1-sulfonic acid (ANS) were also purchased from Sigma-Aldrich. All proteins used in this study were of analytical grade and employed without additional purification[18].

Protein samples were extensively dialyzed against 0.1 M KCl (pH 7.0) at 4 °C to remove low-molecular-weight impurities. Stock protein solutions were passed through 0.22 µm Millipore syringe filters to ensure sample clarity. Protein concentrations were determined spectrophotometrically using a molar extinction coefficient of **1.06×10^5 M^{-1} cm^{-1}** at 409 nm. Cytochrome c was oxidized with 0.01% potassium ferrocyanide prior to dialysis to ensure its oxidized state. All buffers used for optical measurements were prepared with degassed 0.05 M phosphate buffer (pH 7.4)[19].

2.2. UV-visible spectrophotometry

Absorption spectra of cytochrome c samples, with and without TMAO treatment, were recorded using a Jasco V-660 spectrophotometer equipped with a Peltier-based temperature control system, maintained at 37 °C. For general spectral measurements, protein solutions were prepared at a concentration of 15 µM, while a concentration of 50 µM was used for monitoring the 695 nm absorption band. All measurements were performed using quartz cuvettes with a 1.0 cm path length[18,19].

2.3. Peroxidase activity assay

Peroxidase activity of cytochrome c was determined using guaiacol as a chromogenic substrate. The reaction was initiated by the addition of hydrogen peroxide, and the formation of tetraguaiacol was monitored spectrophotometrically at 470 nm. Final assay concentrations were 1 µM cytochrome c, 1 mM guaiacol, and 2 mM hydrogen peroxide (H_2O_2)[18].

2.4. Molecular Docking Studies

The three-dimensional crystal structure of cytochrome c (PDB ID: 1HRC) was retrieved from the Protein Data Bank and prepared using Maestro v11 (Schrödinger, 2017). Protein preparation involved the removal of heteroatoms and crystallographic water molecules, followed by structural optimization and energy minimization with the OPLS-3 force field under physiological pH conditions (pH 7.4)[20]. Binding sites were predicted using SiteMap analysis[33]. Induced Fit Docking (IFD) of TMAO was performed using the Glide module across the 5 predicted sites predicted by SiteMap[21]. The ligand structure of trimethylamine N-oxide (TMAO) was obtained from ChEBI in SDF format, energy-minimized, and processed using LigPrep to account for chirality, tautomeric forms, and ionization states. Docking grids were constructed around the key residues of each binding site, and ligand–protein complexes were ranked based on docking scores and Glide energy. Molecular interactions and binding conformations were visualized using PyMOL [22].

2.5. Molecular Dynamics Simulations

MD simulations were conducted using GROMACS 2022.04 with the CHARMM27 force field [23]. After removing docked ligands and water, the protein-ligand complex was solvated in a triclinic TIP3P water box, neutralized with 10 Na^+ and 19 Cl^- ions [24]. Energy minimization was done using the steepest descent method, followed by equilibration using NVT and NPT ensembles for 5 ns each. The 200 ns production run was analyzed for RMSD, RMSF, radius of gyration (R_g), hydrogen bonding, and SASA. Electrostatics were computed using Particle Mesh Ewald (PME), and LINCS was used for bond constraints. Visualizations were generated using VMD and Chimera [25].

2.6. CD measurements

Circular dichroism (CD) spectra were recorded on a Jasco J-810 spectropolarimeter equipped with a Peltier temperature control unit. Each spectrum represented the average of three accumulations. Protein samples at concentrations of 15–20 µM were used for CD measurements. Quartz cuvettes with 0.1 cm and 1.0 cm path lengths were employed for far-UV and near-UV CD spectra, respectively. Baseline corrections were performed by subtracting the corresponding buffer spectra[18,19].

2.7. Fluorescence measurements

Fluorescence measurements were performed on a PerkinElmer LS 55 spectrofluorimeter using a 3 mm quartz cuvette, with both excitation and emission slit widths set to 10 nm. Protein concentrations were maintained at 3 µM for all experiments. Tryptophan fluorescence was recorded by exciting cytochrome c at 295 nm and collecting emission spectra from 310 to 500 nm. For ANS-binding assays, samples were excited at 360 nm, and emission spectra were acquired between 400 and 600 nm, with ANS maintained at a 16-fold molar excess relative to protein. Baseline correction was performed by subtracting the spectra of corresponding buffer blanks[19].

2.8. Statistical analysis

Statistical analyses were conducted using GraphPad Prism 5.0 (GraphPad Software, San Diego, CA, USA). Comparisons between treated and control groups were performed using one-way ANOVA followed by Tukey's post hoc multiple comparison test. For datasets involving fewer than three groups, an unpaired t-test was applied. Data are presented as mean ± standard error of the mean

(SEM; n = 3) unless otherwise specified. A p-value < 0.05 was considered statistically significant.

3. Result

3.1. TMAO increases the peroxidase activity of Cyt c

In its native state, the heme iron of Cyt c is hexacoordinated and in a low-spin state, with His 18 and Met 80 as axial ligands. This tight coordination blocks access of hydrogen peroxide (H_2O_2) to the heme iron, resulting in very low intrinsic peroxidase activity. However, slight destabilization of the native structure can weaken or break the Met 80 bond to the heme iron, which results in the opening of the heme pocket[26,27]. This allows greater access to the catalytic centre and leads to a significant increase in the peroxidase activity. To assess the effect of TMAO on peroxidase activity, Cyt c was incubated overnight with increasing concentrations of TMAO (50–250 µM), and enzyme activity was measured using guaiacol as substrate. Figure 1a shows the standard absorbance curve at 470 nm measured for 10 minutes and Figure 1b shows the corresponding calculated percent peroxidase activity in a bar diagram with increasing concentrations of TMAO at the end of 10 minutes[28]. A significant increase in peroxidase activity was observed at 50–250 µM TMAO compared with native Cyt c (one-way ANOVA followed by Tukey's post hoc test; $p < 0.005$).

3.2.Effect of TMAO on the structural integrity of Cyt c

To explore the structural basis of the enhanced peroxidase activity, biophysical and spectroscopic analyses were performed to examine the conformational effects of TMAO binding.

Far-UV CD, which reports secondary structure (α-helices give characteristic negative bands at ~208 and 222 nm), showed a clear perturbation in the 208 nm band, indicating altered helical content (Fig. 2a). Tertiary structural rearrangements associated with this secondar structural alteration were studied using Near-UV CD, which revealed a decrease in ellipticity in the 280–290 nm region, consistent with alterations in the local environment of the Trp residue (Fig. 2b). In line with these CD changes, intrinsic Trp fluorescence experiments displayed a marked increase in emission near ~350 nm upon overnight incubation with TMAO, an effect attributable to relief of heme-mediated quenching of the Trp residue in the native state, implying increased separation and/or reduced electronic coupling between Trp and the heme (Fig. 2c). Complementarily, ANS fluorescence exhibited hyperchromicity with a prominent blue shift, indicating binding to newly exposed hydrophobic patches (Fig. 2d). Together, these results indicate that TMAO induces partial unfolding of Cyt c, resulting in secondary and tertiary structural perturbations and exposure of hydrophobic clusters—consistent with the formation of a more flexible, peroxidase-active conformation.

3.3. TMAO binding reduces Heme iron and disrupts the redox status of Cyt c.

To determine whether the TMAO-modified Cyt c corresponds to an apoptotically competent form, the heme absorption spectra of native and TMAO-treated Cyt c were compared (Figure 3a). A significant increase in the heme absorption at 409 nm in the case of TMAO-modified Cyt c was observed as compared to the native unmodified protein, indicative of a conformational change in the heme moiety that results in its increased exposure to the solvent. Comparison of redox spectra revealed that the untreated Cyt c displayed a single broad band at 530 nm, characteristic of the oxidized state, whereas TMAO-treated Cyt c showed a distinct splitting into 520 and 550 nm peaks (Figure 3b). Such splitting is a hallmark of the reduced heme-center, strongly indicating that TMAO binding induces reduction of the heme moiety and thereby alters the redox state of Cyt C.

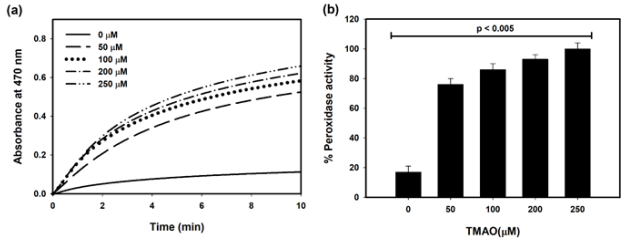

Fig. 1. Peroxidase activity of native and modified Cyt c. (a). Peroxidase activity was assayed using guaiacol as substrate by measuring the increase in absorption at 470 nm for tetraguaiacol formed as product. (b). Bar graph showing percent peroxidase activity in the presence of increasing concentrations of TMAO (50–250 µM). Data are presented as **mean ± SEM (n = 3)**. Statistical analysis was performed using one-way ANOVA followed by Tukey's post hoc test; $p < 0.005$ vs. native Cyt c.

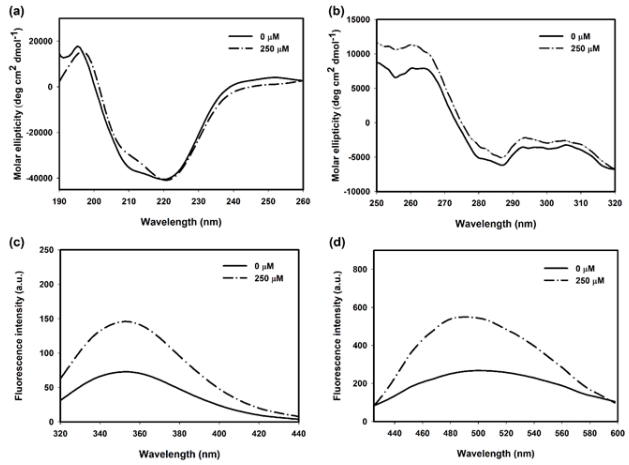

Fig. 2. Effect of TMAO on structural integrity of Cyt c. (a) Far-UV CD spectra, (b) Near-UV CD spectra, (c) Trp and (d) ANS fluorescence spectra of native and TMAO-treated cyt c.

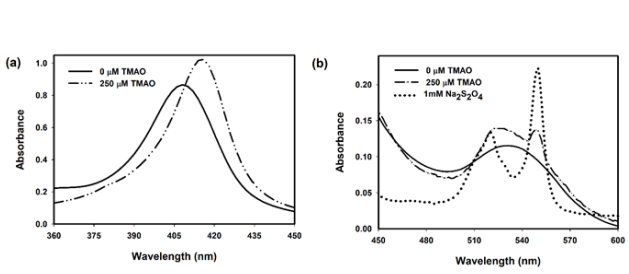

Fig. 3. Effect of TMAO on the Heme moiety of Cyt c. (a) Heme absorption spectra of both native and TMAO-treated protein. (b) redox states of native and modified Cyt c along with a chemically reduced positive control (1 mM $Na_2S_2O_4$).

3.4. TMAO binding disrupts Cyt c Heme-Met80 ligation

In its native state, cytochrome c holds the heme group in a stable hexa-coordinated arrangement, where the sixth ligand is provided by Met 80. This Met 80–heme bond is crucial, as even subtle changes to it can dramatically influence both the structure and function of the protein. When this coordination is disrupted, Cyt C shifts into a less stable penta-coordinated form that acquires peroxidase activity, a function closely linked to its role in apoptosis[29,30]. One of the classic signatures of the Met80 heme interaction is the weak absorption band observed at 695 nm. Loss or weakening of this band reflects the breakage of the Met80 heme bond[31,32]. It is clearly seen in Figure 4 that there is a gradual loss in the 695 nm band after treatment with 250µM TMAO. Thus, TMAO drives Cyt C into such a non-native, penta-coordinated conformation, accompanied by disrupted tertiary interactions, consistent with its conversion into an apoptotically competent species.

3.5. In-vitro binding study using ITC

In order to experimentally validate direct interaction between TMAO and Cyt c, isothermal titration calorimetry (ITC) experiments were performed at 25°C.

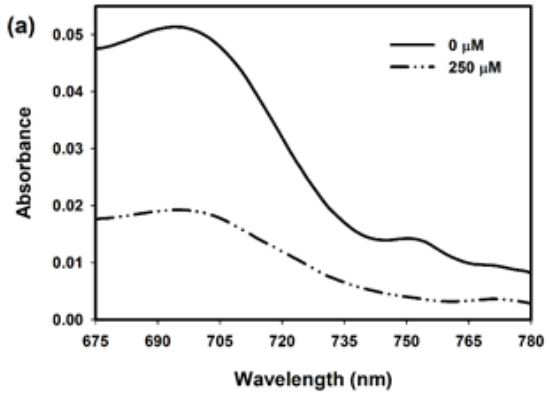

Fig. 4. Effect of TMAO on Cyt c Heme-Met80 ligation. Absorption spectra of untreated and TMAO-treated Cyt c.

TMAO was titrated into a solution of Cyt c (50 µM), and the resulting thermogram and integrated heat data were analyzed using a one-site binding model.

The ITC binding isotherm showed distinct exothermic peaks for each injection, followed by saturation after several titrations (Figure 5a). The integrated binding curve fitted well to a single-site model with a dissociation constant (Kd) of approximately 0.62 mM, indicating a moderate but specific interaction between TMAO and Cyt c. The negative enthalpy change (ΔH = −2.53 kcal/mol) and positive entropy (ΔS = +11.8 cal/mol·K) suggest that the binding process is both enthalpically and entropically favorable, dominated by hydrogen bonding and hydrophobic interactions (Figure 5b).

3.6. TMAO binds to Cyt c

To complement the biochemical data and identify potential binding sites, molecular docking and molecular dynamics (MD) simulations were performed.

First of all, in silico molecular docking studies were performed using Glide module of Schrödinger. Potential ligand binding pockets in the protein were identified using the SiteMap module of Schrödinger. This analysis revealed at least 5 putative binding sites in the protein, with their corresponding residues and site scores listed in Table 1. Systematic Glide docking of TMAO at these individual sites yielded binding energies ranging from −9.4 to −25.6 kcal/mol (Table 2). According to the Glide 6.7

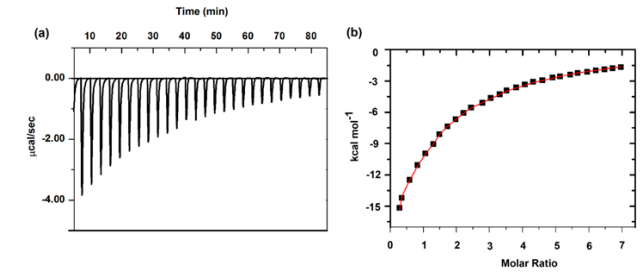

Fig. 5. In-vitro binding analysis using ITC. (a) Time-dependent thermogram upon injection with different concentrations of TMAO. (b) Resultant binding isotherm prior to the integration of peak area and normalization to yield a plot of molar enthalpy change against control Cytochrome c-TMAO ratio.

Table 1. List of different pockets along with their amino acid and site score obtained from site map analysis.

Site number	amino acid	SiteScore
Site 1	Lys99, Ile 95, Phe36	0.90
Site 2	Lys5, Ile9, Gln12	0.88
Site 3	Thr 19, Val 20, His18	0.84
Site 4	Gly 56, ILE57, Asn54	0.76
Site 5	Pro71, Asn70, Glu69	0.61

Table 2. Values of docking score (unitless) and glide energy (kcal/mol) of the binding interaction between the pockets of Cyt c and TMAO.

Site number	Docking Score	Glide energy
Site 1	-5.2	-25.6
Site 2	-4.3	-21.6
Site 3	-3.9	-14.2
Site 4	-3.5	-13.1
Site 5	-3.3	-9.4

documentation, Glide Energy values are reported in kcal/mol, while Docking Score remains a unitless composite docking score; therefore, the values presented in Table 2 adhere to this convention

Notably, the values of docking score and Glide energies were the highest for Site 1 (Glide energy−25.6 kcal/mol; docking score −5.2), indicative of the binding of TMAO in this site. Figures 6a and 6b display the 2D and 3D binding poses of TMAO at this site, along with interactions with the key residues Lys99, Ile95, Glu61and Phe36 of the site. To assess the stability of this interaction, 200 ns molecular dynamics (MD) simulations were performed. RMSD plots obtained indicated that both free and TMAO-bound Cyt c reached equilibrium early and remained stable throughout, with a minor increase of 0.1 Å in average RMSD upon TMAO binding (Figure 6C). RMSF analysis showed enhanced flexibility near residue numbers 25-28, 35-45, 78-82 and 95-102 in the TMAO-bound complex, which clearly indicates the perturbation around key residues of binding site (Figure 6d). Radius of gyration (R_g) values suggested slight expansion of the TMAO-bound protein (Figure 6e), with a concomitant minor variation in the solvent-accessible surface area (SASA), indicating that expansion also affects solvation properties (Figure 6f). Hydrogen bond analysis showed the presence of 1 consistent hydrogen bond throughout the simulation, with bond lengths fluctuating between 1.80 and 1.92 Å (Figure 6g and 6h). Collectively, these results confirm that TMAO binds to Cyt C and also induces modest structural flexibility.

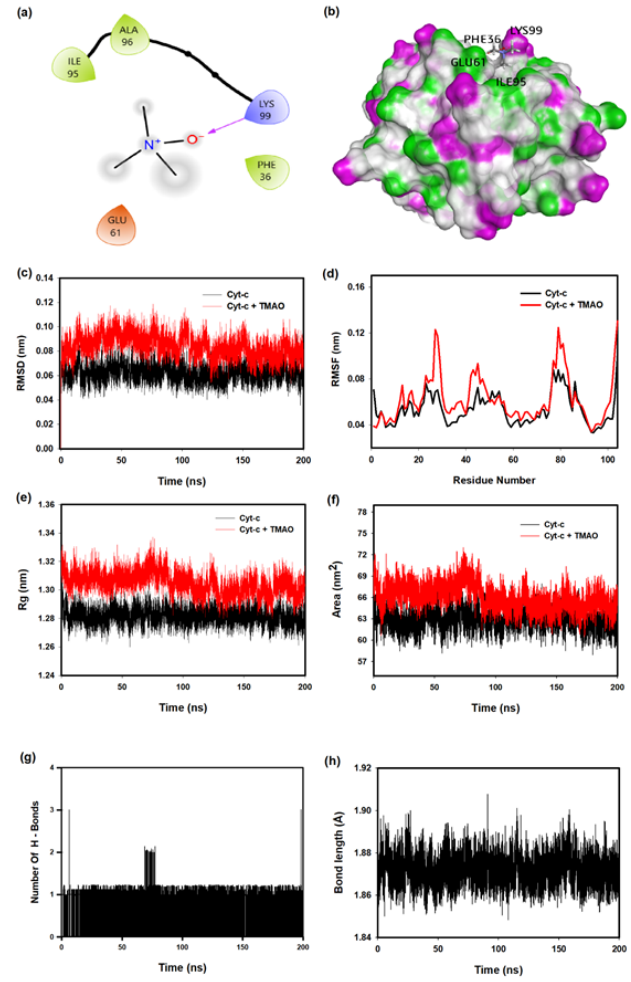

Fig. 6. In silico molecular docking and molecular dynamics simulation studies showing binding of TMAO to the Cytochrome c. (a) 2D ligand interaction diagram of TMAO bound near the Lys 99 of Cytochrome c. (b) 3D graphical representation of TMAO bound near the Lys 99 of Cytochrome c. (c) The RMSD plot showing the changes between the stabilities in the observed systems. (d) The graphical representation of the changes observed in the fluctuation of the constituent residues between the TMAO-bound and unbound Cytochrome c. (e) The Rg plots showing the difference in the compactness between the TMAO bound and unbound Cyt c. (f) The graphical representation of the changes observed in the Solvent accessible surface area (SASA) between the TMAO-bound and unbound Cyt c. (g) Hydrogen-bond fluctuations plot highlighting the changes in the observed number. (h) Fluctuations in the hydrogen-bond length throughout the run.

4. Discussion

Our study reveals, for the first time, that the gut microbiota–derived metabolite trimethylamine N-oxide (TMAO) directly alters the structural and functional integrity of cytochrome c (Cyt c), converting it into an apoptotically competent species. In its native conformation, Cyt c exists as a hexa-coordinated, low-spin heme protein with Met80 and His18 serving as axial ligands[34]. This coordination effectively shields the heme iron from reactive oxygen species and maintains low basal peroxidase activity. Our results show that TMAO treatment disrupts this protective arrangement, as evidenced by the loss of the diagnostic 695 nm absorption and a parallel gain in peroxidase activity. These findings align with previous reports on other metabolite-induced Cyt c modifications, such as N-homocysteinylation [19] and glyoxal-induced glycation [18], which similarly convert Cyt c into a penta-coordinated peroxidase-active species. The concentrations used here (50–250 µM) fall within the range observed in pathological states such as atherosclerosis, chronic kidney disease, and metabolic syndrome. This ensures that the structural and functional effects we observed reflect clinically relevant exposures rather than supraphysiological artifacts[35]. However, unlike covalent modifications that require chemical adduct formation, the effect of TMAO arises from non-covalent binding, underscoring a novel mechanism of structural perturbation. Molecular docking and MD simulations further revealed that TMAO binds stably near Lys99 through hydrogen bonding, inducing local flexibility and subtle expansion of the protein structure. This binding event correlates with spectroscopic evidence of altered tertiary packing (near-UV CD, Trp fluorescence) and increased solvent exposure of hydrophobic residues (ANS binding). Importantly, heme absorbance measurements indicated that TMAO-modified Cyt c undergoes reduction of its iron center, shifting its redox state and enabling enhanced catalytic activity toward guaiacol in the presence of H_2O_2. Together, these structural and functional alterations define a non-native Cyt c species that is both redox-active and apoptotically competent. Similar non-native Cyt c conformers with exposed heme and enhanced peroxidase activity have been described during cardiolipin interaction[36] and upon chemical modification [18,19]. The transition of Cyt c to a peroxidase-active state is a decisive event in apoptosis, as peroxidase activity catalyzes oxidation of mitochondrial cardiolipin—a prerequisite for Cyt c detachment from the inner mitochondrial membrane and its release into the cytosol[37]. By promoting heme exposure and redox disruption, TMAO effectively primes Cyt c for this release. Thus, our findings extend the pro-apoptotic repertoire of TMAO from ER stress and inflam-

masome pathways to direct modulation of mitochondrial death machinery. This provides a missing mechanistic link between elevated circulating TMAO, mitochondrial dysfunction, and apoptotic cell loss in cardiovascular and metabolic disorders.

A particularly striking feature of our results is the paradoxical behavior of TMAO. While TMAO is classically described as an osmolyte that stabilizes proteins under stress [38], our data indicate that in the case of Cyt c, TMAO destabilizes tertiary contacts and weakens axial heme ligation. This duality suggests that TMAO's effects are protein-context dependent, stabilizing some proteins while rendering others apoptotically competent. Such specificity may help explain why systemic TMAO elevation is associated with broad tissue injury, from vascular apoptosis to renal and metabolic dysfunction[39]. Taken together, we propose that TMAO binding converts native Cyt c into a structurally destabilized, redox-active, peroxidase-competent form. This remodeled Cyt c can accelerate mitochondrial lipid oxidation, facilitate release from the mitochondrial membrane, and engage the intrinsic apoptotic pathway. By directly targeting Cyt c at the critical heme–Met80 coordination switch, TMAO emerges as a potent modulator of mitochondrial cell death, providing a unifying mechanistic insight into its pathological associations. This mechanistic cascade is illustrated in Figure 7, which summarizes the sequence of events from TMAO binding at the Lys99 region to structural perturbation, Met80–heme disruption, enhanced peroxidase activity, cardiolipin oxidation, and eventual cytochrome c release leading to apoptosis. While the loss of the 695 nm band and splitting of the 530 nm band into 520 and 550 nm strongly suggest disruption of the Met80–heme ligation and heme reduction, respectively, these results are correlative and based on spectroscopic evidence. Advanced confirmation through resonance Raman, EPR, or redox titration should be carried out in future work. It should also be noted that the study employed bovine Cyt c, which shares over 90% sequence identity with the human protein. Both the proposed TMAO-binding residues (Lys99, Ile95, Glu61, Phe36) and active-site residues (His18, Met80, Tyr67, Thr78, Lys72) are fully conserved, supporting the general relevance of our findings to human Cyt c[34]. Future in vivo studies are warranted to establish whether this mechanism operates under physiological concentrations of TMAO and contributes directly to disease pathogenesis. Targeting the TMAO–Cyt c axis may thus represent a promising therapeutic strategy to mitigate TMAO-driven cardiovascular and metabolic disorders. While TMAO has been widely associated with endoplasmic reticulum (ER) stress, inflammasome activation, and metabolic dysfunction [36], its ability to act directly on the mitochondrial apoptotic machinery has remained largely unexplored. Here, we demonstrate that TMAO binding destabilizes the heme–Met80 ligation of Cyt c, disrupts its tertiary structure, exposes the heme pocket, and enhances peroxidase activity—molecular hallmarks of Cyt c's shift from an electron carrier to a pro-apoptotic catalyst. The underlying mechanisms of many TMAO-related pathologies converge on oxidative stress, inflammatory signalling, and mitochondrial damage. Our findings extend this view by showing that TMAO can also drive apoptosis through its direct impact on cytochrome c. Notably, TMAO distribution in the body is organ-dependent, with its concentrations being higher in tissues where O_2 transporters are upregulated[40]. This tissue-specific enrichment may help explain why organs such as the kidney and liver sites of chronic kidney disease (CKD) and non-alcoholic fatty liver disease (NAFLD), respectively, exhibit pronounced TMAO-associated toxicity. In these contexts, elevated TMAO may sensitize cells to apoptosis by destabilizing cytochrome c, thereby amplifying tissue injury and disease progression.

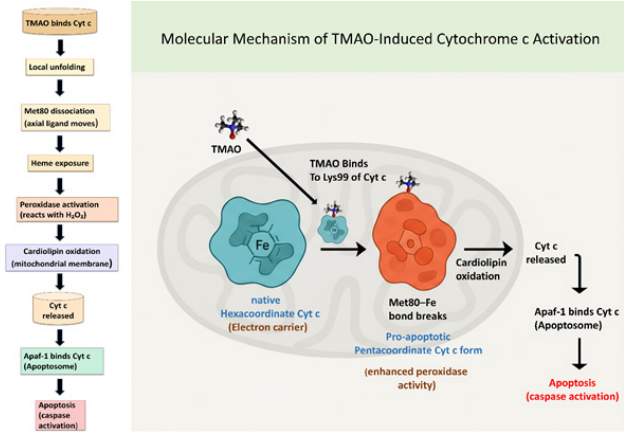

Fig. 7. Schematic representation of the TMAO–Cytochrome c apoptotic mechanism.

Conflict of Interest

The authors declare that they have no conflicts of interest with the contents of this article.

Acknowledgements

Funding: This work is partly supported by grants from DU-IOE [IOE/2024-2025/12/FRP] provided to LRS, CSIR-SRA [13(9259-A)/2023-POOL] provided to AG and CSIR-UGC (F-03/19-20/16) to KS.

Author's Contribution: KS, AK, SY, NM, PR and KM performed the experiments and assisted in the computational work. KS, AG and LRS conceived the idea and analyzed the data. KS, AG and LRS wrote the manuscript.

Consent for publications

All authors have read and approved the final manuscript for publication.

Availability of data and material

We have embedded all data in the manuscript.

References

1. Koeth RA, Wang Z, Levison BS, Buffa JA, Org E, Sheehy BT, et al. (2013) Intestinal microbiota metabolism of L-carnitine, a nutrient in red meat, promotes atherosclerosis. Nat Med 19: 576–585 doi: 10.1038/nm.3145
2. Zhen J, Zhou Z, He M, Han HX, Lv EH, Wen PB, et al. (2023) The gut microbial metabolite trimethylamine N-oxide and cardiovascular diseases. Front Endocrinol (Lausanne) 14: 1085041 doi: 10.3389/fendo.2023.1085041
3. Chhibber-Goel J, Singhal V, Parakh N, Bhargava B, Sharma A. The metabolite trimethylamine-N-oxide is an emergent biomarker of human health. EurekaSelect [Internet]. Available from: http://www.eurekaselect.com

4. Swanepoel I, Roberts A, Brauns C, Chaliha DR, Papa V, Palmer RD, et al. (2022) Trimethylamine N-oxide (TMAO): a new attractive target to decrease cardiovascular risk. Postgrad Med J 98: 723–727 doi: 10.1136/postgradmedj-2021-139839
5. Konieczny R, Kuliczkowski W (2023) Trimethylamine N-oxide in cardiovascular disease. Adv Clin Exp Med 31: 913–925 doi: 10.17219/acem/147666
6. Caradonna E, Abate F, Schiano E, Paparella F, Ferrara F, Vanoli E, et al. (2025) Trimethylamine-N-oxide (TMAO) as a rising-star metabolite: Implications for human health. Metabolites 15: 220 doi: 10.3390/metabo15040220
7. Constantino-Jonapa LA, Espinoza-Palacios Y, Escalona-Montaño AR, Hernández-Ruiz P, Amezcua-Guerra LM, Amedei A, et al. (2023) Contribution of trimethylamine N-oxide (TMAO) to chronic inflammatory and degenerative diseases. Biomedicines 11: 431 doi: 10.3390/biomedicines11020431
8. Canyelles M, Borràs C, Rotllan N, Tondo M, Escolà-Gil JC, Blanco-Vaca F (2023) Gut microbiota-derived TMAO: A causal factor promoting atherosclerotic cardiovascular disease? Int J Mol Sci 24: 1940 doi: 10.3390/ijms24031940
9. Zhou Y, Zhang Y, Jin S, Lv J, Li M, Feng N (2024) The gut microbiota derived metabolite trimethylamine N-oxide: Its important role in cancer and other diseases. Biomed Pharmacother 177: 117031 doi: 10.1016/j.biopha.2024.117031
10. Kumari K, Warepam M, Bansal AK, Singh LR (2023) Trimethylamine N-oxide modulates carbonic anhydrase folding landscape and catalytic activity. Arch Biochem Biophys 732: 109497 doi: 10.1016/j.abb.2023.109497
11. Martelli A, Abate F, Roggia M, Benedetti G, Caradonna E, Calderone V, et al. (2025) Trimethylamine N-oxide (TMAO) acts as inhibitor of endothelial nitric oxide synthase (eNOS) and hampers NO production and acetylcholine-mediated vasorelaxation in rat aortas. Antioxidants (Basel) 14: 517 doi: 10.3390/antiox14050517
12. Singh N, Mondal S, Goswami S, Chaturvedi N (2023) Interaction studies unveil potential binding sites on bovine serum albumin for gut metabolite trimethylamine N-oxide (TMAO). BMC Chem 17: 80 doi: 10.1186/s13065-023-00498-2
13. Fiorucci L, Erba F, Santucci R, Sinibaldi F (2022) Cytochrome c interaction with cardiolipin plays a key role in cell apoptosis: Implications for human diseases. Symmetry 14: 767 doi: 10.3390/sym14040767
14. Hanske J, Toffey JR, Morenz AM, Bonilla AJ, Schiavoni KH, Pletneva EV (2012) Conformational properties of cardiolipin-bound cytochrome c. Proc Natl Acad Sci U S A 109: 125–130 doi: 10.1073/pnas.1112310108
15. Santucci R, Sinibaldi F, Patriarca A, Santucci D, Fiorucci L (2010) Misfolded proteins and neurodegeneration: Role of non-native cytochrome c in cell death. Expert Rev Proteomics 7: 507–517 doi: 10.1586/epr.10.50
16. Garrido C, Galluzzi L, Brunet M, Puig PE, Didelot C, Kroemer G (2006) Mechanisms of cytochrome c release from mitochondria. Cell Death Differ 13: 1423–1433 doi: 10.1038/sj.cdd.4401950
17. Jiang X, Wang X (2004) Cytochrome c-mediated apoptosis. Annu Rev Biochem 73: 87–106 doi: 10.1146/annurev.biochem.73.011303.073706
18. Sharma GS, Warepam M, Bhattacharya R, Singh LR (2019) Covalent modification by glyoxals converts cytochrome c into its apoptotically competent state. Sci Rep 9: 4781 doi: 10.1038/s41598-019-41282-2
19. Sharma GS, Singh LR (2017) Conformational status of cytochrome c upon N-homocysteinylation: Implications to cytochrome c release. Arch Biochem Biophys 614: 23–27 doi: 10.1016/j.abb.2016.12.006
20. Sastry GM, Adzhigirey M, Day T, Annabhimoju R, Sherman W (2013) Protein and ligand preparation: Parameters, protocols, and influence on virtual screening enrichments. J Comput Aided Mol Des 27: 221–234 doi: 10.1007/s10822-013-9644-8
21. Halgren TA, Murphy RB, Friesner RA, Beard HS, Frye LL, Pollard WT, et al. (2004) Glide: A new approach for rapid, accurate docking and scoring. 2. Enrichment factors in database screening. J Med Chem 47: 1750–1759 doi: 10.1021/jm030644s
22. Schrödinger, LLC (2015) The PyMOL Molecular Graphics System, Version 2.0.
23. Van Der Spoel D, Lindahl E, Hess B, Groenhof G, Mark AE, Berendsen HJC (2005) GROMACS: Fast, flexible, and free. J Comput Chem 26: 1701–1718 doi: 10.1002/jcc.20291
24. Jo S, Kim T, Iyer VG, Im W (2008) CHARMM-GUI: A web-based graphical user interface for CHARMM. J Comput Chem 29: 1859–1865 doi: 10.1002/jcc.20945
25. Humphrey W, Dalke A, Schulten K (1996) VMD – Visual Molecular Dynamics. J Mol Graph 14: 33–38 doi: 10.1016/0263-7855(96)00018-5
26. Yin V, Shaw GS, Konermann L (2017) Cytochrome c as a peroxidase: Activation of the precatalytic native state by H2O2-induced covalent modifications. J Am Chem Soc 139: 15701–15709 doi: 10.1021/jacs.7b07106
27. Birk AV, Chao WM, Liu S, Soong Y, Szeto HH (2015) Disruption of cytochrome c heme coordination is responsible for mitochondrial injury during ischemia. Biochim Biophys Acta Bioenerg 1847: 1075–1084 doi: 10.1016/j.bbabio.2015.06.006
28. Chea EE, Deredge DJ, Jones LM (2020) Insights on the conformational ensemble of cytochrome c reveal a compact state during peroxidase activity. Biophys J 118: 128–137 doi: 10.1016/j.bpj.2019.11.011
29. Belikova NA, Vladimirov YA, Osipov AN, Kapralov AA, Tyurin VA, Potapovich MV, et al. (2006) Peroxidase activity and structural transitions of cytochrome c bound to cardiolipin-containing membranes. Biochemistry 45: 4998–5009 doi: 10.1021/bi0525573
30. Basova LV, Kurnikov IV, Wang L, Ritov VB, Belikova NA, Vlasova II, et al. (2007) Cardiolipin switch in mitochondria: shutting off the reduction of cytochrome c and turning on the peroxidase activity. Biochemistry 46: 3423–3434 doi: 10.1021/bi061854k
31. Boon EM, Downs AM, Kim J, Marletta MA (2004) Characterization of the nitrite reductase activity of met-oxidized cytochrome c. Biochemistry 43: 11331–11339 doi: 10.1021/bi049028j
32. Santucci R, Ascoli F (1997) The Soret circular dichroism spectrum as a probe for the heme Fe(III)-Met(80) axial bond in horse cytochrome c. J Inorg Biochem 68: 211–214 doi: 10.1016/s0162-0134(97)00100-1
33. Halgren TA (2009) Identifying and characterizing binding sites and assessing druggability. J Chem Inf Model 49: 377–389 doi: 10.1021/ci800324m
34. Alvarez-Paggi D, Hannibal L, Castro MA, Oviedo-Rouco S, Demicheli V, Tórtora V, et al. (2017) Multifunctional cytochrome c: learning new tricks from an old dog. Chem Rev 117: 13382–13460 doi: 10.1021/acs.chemrev.7b00257
35. Stubbs JR, Hogue CW, Ocque AJ, et al. (2015) Serum trimethylamine-N-oxide is elevated in chronic kidney disease and correlates with atherosclerosis in CKD patients. PLoS One 11: e0141738 doi: 10.1371/journal.pone.0141738
36. Chen S, Henderson A, Petriello MC, Romano KA, Gearing M, Miao J, et al. (2019) Trimethylamine N-oxide binds and activates PERK to promote endoplasmic reticulum stress and metabolic dysfunction. JCI Insight 4: e123970 doi: 10.1172/jci.insight.123970

37. Kagan VE, Tyurin VA, Jiang J, Tyurina YY, Ritov VB, Amoscato AA, et al. (2005) Cytochrome c acts as a cardiolipin oxygenase required for release of proapoptotic factors. Nat Chem Biol 1: 223–232 doi: 10.1038/nchembio727
38. Yancey PH (2005) Organic osmolytes as compatible, metabolic and counteracting cytoprotectants in high osmolarity and other stresses. J Exp Biol 208: 2819–2830 doi: 10.1242/jeb.01730
39. Tang WHW, Wang Z, Levison BS, Koeth RA, Britt EB, Fu X, et al. (2013) Intestinal microbial metabolism of phosphatidylcholine and cardiovascular risk. N Engl J Med 368: 1575–1584 doi: 10.1056/NEJMoa1109400
40. Wang Z, Man S, Koeth R (2025) TMAO metaorganismal pathway and chronic inflammatory diseases. Explor Med 6: 1001339 doi: 10.37349/emed.2025.1001339